2021 13th International Conference on Information & Communication Technology and System (ICTS) | 978-1-6654-4059-2/21/$31.00 ©2021 IEEE | DOI: 10.1109/ICTS52701.2021.9608854

Automatic Segmentation of Optic Nerve Head by Median Filtering and Clustering Approach

Anindita Septiarini
Department of Informatics
Faculty of Engineering
Mulawarman University
Samarinda, Indonesia
anindita@unmul.ac.id

Hamdani Hamdani
Department of Informatics
Faculty of Engineering
Mulawarman University
Samarinda, Indonesia
hamdani@unmul.ac.id

Emy Setyaningsih
Department of Computer
System Engineering
Institut Sains Teknologi AKPRIND
Yogyakarta, Indonesia
emysetyaningsih@akprind.ac.id

Edwanda Arisandy
Department of Informatics
Faculty of Engineering
Mulawarman University
Samarinda, Indonesia
edwandasandy@gmail.com

Suyanto Suyanto
School of Computing
Telkom University
Bandung, Indonesia
suyanto@telkomuniversity.ac.id

Edy Winarno
Faculty of Information Technology
Universitas Stikubank
Semarang, Indonesia
edywin@edu.unisbank.ac.id

***Abstract*—The optic nerve head (ONH) is a sphere area with light-colored on the fundus image. It needs to be observed by an ophthalmologist to detect glaucoma. Glaucoma is an eye disease that may cause permanent blindness. It can be detected based on the cup-to-disk ratio (CDR) value. This value is generated by calculating the diameter length of the ONH. In order to perform these calculations, it is necessary to segment the ONH area. This study aims to develop an ONH area segmentation method that consists of four main processes: detection of the region of interest (ROI), pre-processing, segmentation and post-processing. ROI detection is implemented in the green channel using the OTSU method, followed by pre-processing using the median filtering, which aims to discard the blood vessel. Furthermore, K-Means is applied to the segmentation process, followed by post-processing using several morphological operations to remove the appearance noise. This method successfully achieves the $F1_{score}$ value of 0.941 with test data of 68 images.**

***Index Terms*—Segmentation, blood vessels removal, median filter, clustering, K-Means**

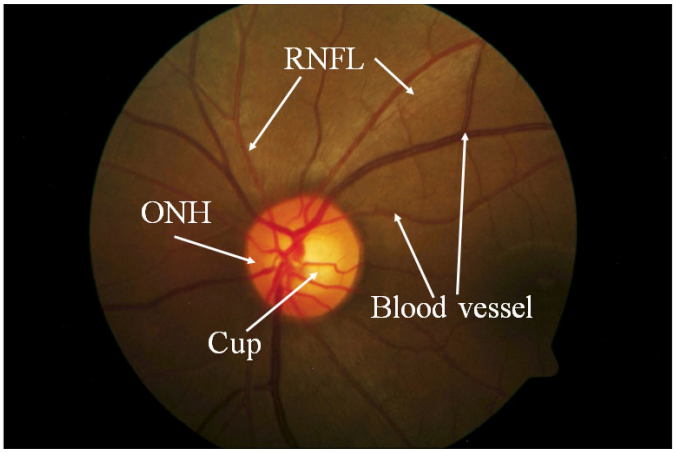

Fig. 1. The structure of a fundus image

I. Introduction

The optic nerve head (ONH) is an elliptical light-colored area in the fundus image. In addition, other parts on the fundus image that can be observed are blood vessel, cup, and retinal nerve fiber layer (RNFL). Blood vessels are reddish-colored parts that are placed in the outer and inner areas of the ONH. Meanwhile, the cup is a spherical area located inside the ONH. It has a lighter color than ONH. Furthermore, the RNFL is the part that looks like a white streak outside the ONH. An example of the fundus image structure is shown in Fig. 1.

Fundus images are used by ophthalmologists to diagnose diseases, one of which is glaucoma. Glaucoma is the second leading and incurable disease causing blindness in the world [1]. This disease was detected based on the value of the cup-to-disc ratio (CDR) and the thickness of the RNFL. In normal eyes, the CDR value is ± 0.3 which is obtained from the calculation of the vertical diameter value of the cup and disc (refer to ONH). Meanwhile, in normal eyes, the RNFL tends to be thick and clearly visible in the entire area outside the ONH. Moreover, the blood vessels tend to be covered by RNFL [2]. Actually, the calculation of the CDR value and the thickness detection of the RNFL can be done manually by ophthalmologists. Still, the results become subjective because psychological conditions influence them, especially if the observations are deal with large amounts of data. In order to overcome this case, several studies related to calculating the CDR value [3]–[6], detection of thickness RNFL [7]–[11], peripapillary atrophy detection [12], and glaucoma detection [13]–[16] have been developed. Those works

required the ONH segmentation process. In calculating the CDR value, ONH segmentation is needed to produce the vertical diameter value. Meanwhile, in RNFL detection, the ONH area needs to be discarded because the presence of the RNFL is outside it. Therefore, the ONH segmentation process must be applied.

In previous studies, to obtain optimal ONH segmentation results in fundus images, a blood vessel removal process was needed. This process aims to remove the blood vessel area, hence the ONH boundaries are more clearly visible. Several blood vessel removal methods have been implemented i.e. clustering [17], [18], curve-fitting technique [19], Gaussian filter [20] and Sparse-Based inpainting [21]. The ONH area was easier to distinguish from the background by implementing the segmentation method in a certain channel of color space such as red [5], [22] and green [23]. The study of ONH segmentation is still being developed. There are several methods that have been used, including thresholding [24]–[26], active contour [27], [28], hough transform [29], [30], wavelet [31], region growing [19], clustering [23].

The contribution of this study is in developing the ONH segmentation method. It was applied in the red color space by implementing median filtering combined with clustering with the K-Means algorithm. This method is robust against the local dataset used and can produce high segmentation accuracy.

II. Materials and Methods

The local dataset used in this study was provided by Dr. YAP Eye Hospital in Yogyakarta, Indonesia. Nikon N150 digital camera combined with a 30° FOV Carl Zeiss AG fundus camera acquired 68 retinal fundus images. Those images are saved in JPEG format with a resolution of 2240×1488 pixels. As a need for the performance evaluation of the proposed method, ophthalmologists with experience of 10 years will make a ground truth. The first row in Fig. 2 shows the examples of fundus image from the local dataset, and the second row presents the ground truths. In the evaluation process, the ground truths convert into a binary image.

This study aims to determine the area of ONH and background. The input is a fundus image, while the output is an image that is only the ONH area. The proposed method consists of four main processes: 1) region of interest (ROI) detection, 2) pre-processing, 3) segmentation, and 4) post-processing. The evaluation process is carried out to test the performance of the proposed method based on the segmentation result area. The overview of the stages of the process of the proposed method is illustrated in Fig. 3.

A. ROI detection

The process of ROI detection aims to produce a sub-image (called the ROI image), focusing on the ONH area. Therefore, it can reduce the computation time at the following stage. This process begins with finding the ONH center by applying thresholding using the Otsu method, with the threshold value is 1/5 of the highest intensity value. Thresholding is implemented in the green channel because the cup area has the highest intensity value, which is located in the ONH. This channel makes the cup area more clearly distinguished from other objects [22]. Afterward, the estimated area of ONH was set based on the result of the thresholding. Since the ONH location and the distribution of intensity values on the fundus image vary, the dimension of the ROI image formed varies.

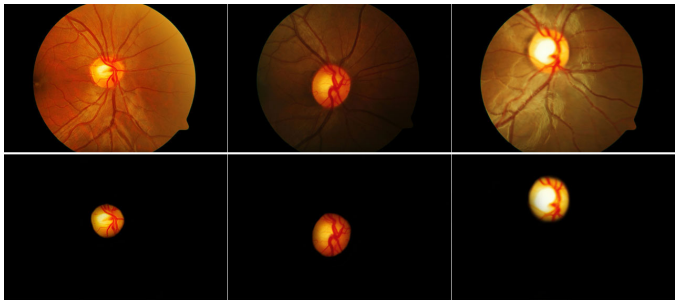

Fig. 2. The examples of fundus image and the ground truths

B. Pre-processing

In this work, pre-processing aims to eliminate the presence of blood vessels covering the area or boundary of the ONH. This causes the ONH area can be detected as a background or vice versa. This process initiated by converting the ROI image in RGB color space to a grayscale image followed by applying median filtering to reduce the appearance of a blood vessel as in [32]. Based on experiments, the use of a 3×3 kernel in the median filtering makes the appearance of the blood vessel more subtle. The examples of ROI images and the results of applying median filtering are shown in Fig. 4 on the first and second columns, respectively.

C. Segmentation

The segmentation process is aimed to distinguish the image into two parts: the ONH area and background. In this study, backgrounds are all other objects outside the ONH area. Segmentation is applied using the K-Means clustering method. It is used because successfully implemented in several studies with medical image data [33]–[35]. The number of clusters (K) = 2 is based on the aim of this process. The algorithm of K-Means defined as follow [35] with:

- Step 1: Initialize cluster centroids (Ci) with the number of k random samples.
- Step 2: Assign each data (x_i) to the nearest cluster center N data $X(x_1, x_2, \ldots, x_n)$ classified by K-means into K clusters using the distance function defined as follow (1):

$$Distance = \sum_{i=1}^{k} \sum_{j=1}^{n} x_{ij} - C_i^2 \tag{1}$$

- Step 3: Step 3: Update each cluster center by recalculating C_i, which is defined as follows(2):

$$C_i = \frac{1}{N_i} \sum_{x \in x_i} x, i = 1, 2, ..., k \tag{2}$$

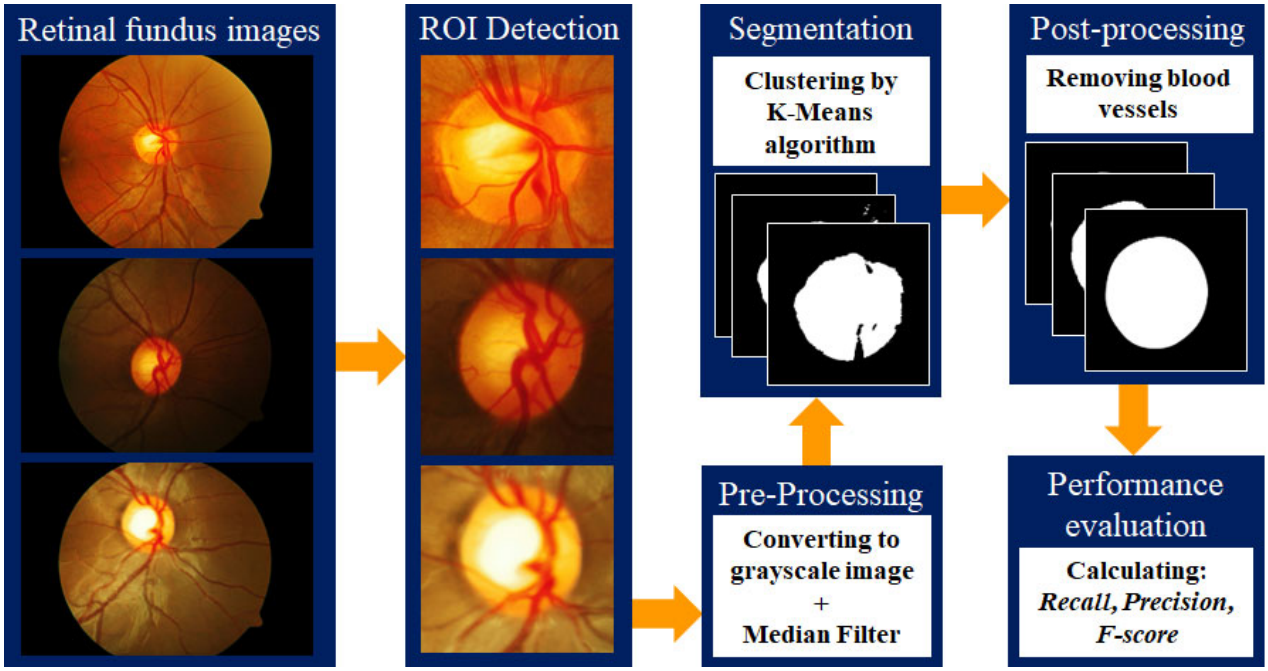

Fig. 3. The main process of the proposed methods

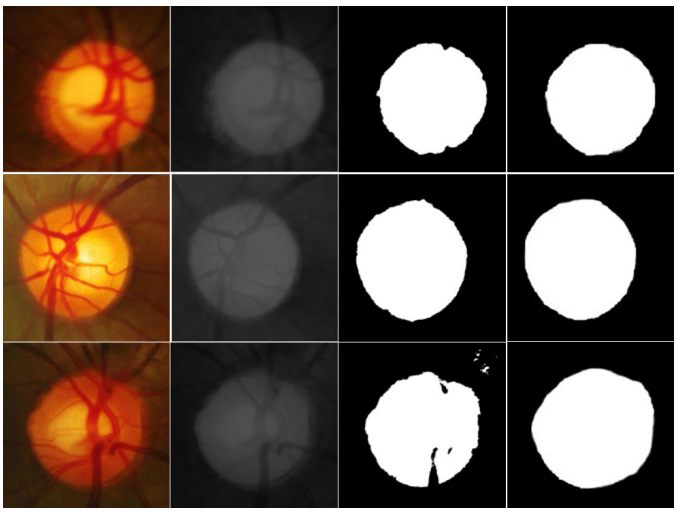

Fig. 4. The resulting images of each process: ROI detection, pre-processing, segmentation, and post-processing

where N_i is the number of elements in the i_{th} cluster.

- Step 4: Repeat steps 2 and 3 until the value of C_i does not change.

Several examples of the segmentation result using the K-means algorithm is depicted in Fig. 4 of the third column. The result of segmentation shows that there is still noise outside ONH. Generally, it occurs because the blood vessel area and the ONH area covered by blood vessels are incorrectly classified as background. The misclassification examples are shown in Fig. 4 (see the third column and row).

D. Post-processing

Post-processing is needed to overcome the misclassification due to the occurrence of blood vessels. This process is implemented using morphology operation. The operations used are erosion, closing, and dilation. Firstly, erosion is applied by the strel size 10, which aims to discard the noise outside the ONH area. Furthermore, the closing was applied by the strel size 20 to close the open ONH area. Lastly, due to erosion caused the ONH size becomes smaller; therefore, a dilation operation is applied by the strel size 10. The result of post-processing is shown in Fig. 4 of the fourth column.

E. Performance evaluation based on area

In this study, the performance evaluation was conducted based on area. It is measured by calculating the overlapping area of the white ONH pixels on the ground truth image and the resulting image produced by the method. The performance measures used $recall$, $precision$, and $F1_{score}$ were defined as [5], [27]:

$$Precision = \frac{TP}{TP + FP}, \tag{3}$$

$$Recall = \frac{TP}{TP + FN}, \tag{4}$$

$$F1_{score} = 2 \times \frac{Precision \times Recall}{Precision + Recall}. \tag{5}$$

True positive (TP) is the number of pixels, which is the ONH area of the ground truth image and method. Meanwhile, false positive (FP) is the number of pixels in the method image, which is the ONH area, but the ground truth image is the background. In contrast, the false negative (FN) is the number

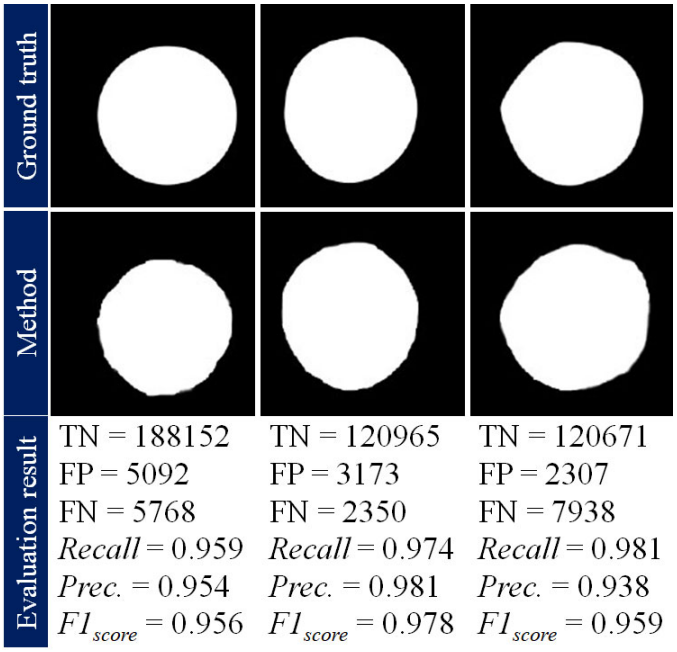

Fig. 5. The resulting examples of performance evaluation

of pixels in the ground truth image, which is the ONH area, but the method image is the background. The performance calculation result of the ONH area segmentation method is shown in Fig. 5. The first line in Fig. 5 shows the ground truth image resulting from manual segmentation performed by an ophthalmologist, the second line is the segmentation result image of the applied method, and the third line shows the value of the performance evaluation results. The performance results lie between 0 and 1. It indicated has good performance if $recall$, $precision$, and $F1_{score}$ values approach 1.

III. Result and Discussion

The evaluation performance in this study was carried out using three segmentation methods and two different filtering methods to produce the optimal result. The segmentation process applied is the iteration method, Otsu, and K-Means, while the filtering method applied is the mean and median. Several test scenarios and their results are shown in Fig. 6.

Fig 6 shows that the median filtering performance is better than the mean filtering. This is indicated by the results of applying the median filtering together with the iteration segmentation method, Otsu, and K-Means, achieving Fscose values of 0.844, 0.930, and 0.941, respectively, exceeding the results of applying the mean filtering of 0.823, 0.907, and 0.916. It is concluded that the best method is to combine K-Means and median filtering. These two methods can produce the highest $F1_{score}$ value of 0.941.

Based on the experiments conducted, there are several insights obtained. The segmentation results that achieve a high $F1_{score}$ value have a clear ONH border, in contrast to the unclear boundaries of ONH resulting in misclassification. Discrepancies in the acquisition process cause the unclear

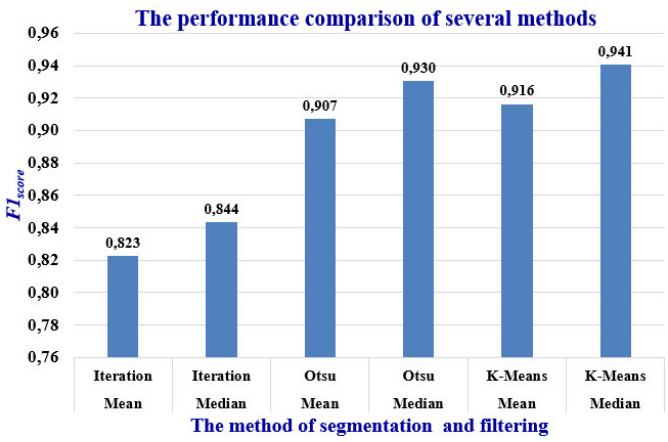

Fig. 6. The performance comparison of several methods

boundaries of the ONH. Meanwhile, the appearance of the main blood vessel covering the ONH area, especially the edges, also caused the erroneous segmentation result.

IV. Conclusion

This study proposes the ONH segmentation method by applying the median filtering and K-Means followed by morphology operation to remove the noise. The performance of this method was tested using several 68 fundus images by calculating the $F1_{score}$ value. The performance evaluation results show that the proposed method can achieve the $F1_{score}$ value of 0.941. The segmentation misclassification occurs; hence the process of image acquisition is not appropriate, which causes the ONH boundaries to become unclear. In addition, the ONH boundaries covered by the main blood vessel resulted in misclassification due to the ONH area classified into the background area. The erroneous that occurred in this study is still very likely to be corrected. Development can be carried out at the pre-processing and blood vessel removal process stages to obtain a more significant difference between the ONH and background areas. In addition, the segmentation method needs to be developed to reduce the appearance of noise.

Acknowledgment

The authors would like to thank Dr. YAP Eye Hospital in Yogyakarta, Indonesia, which has provided the private datasets, and KEMENDIKBUD RISTEK Indonesia in 2021 for supporting the funding (Grant no. 594/UN17.11/PG/2021).

References

[1] H. A. Quigley and A. T. Broman, "The number of people with glaucoma worldwide in 2010 and 2020," *British Journal of Ophthalmology*, vol. 90, no. 3, pp. 262–267, 2006.

[2] G. Holló, "The Optic Nerve in Glaucoma," in *Atlas of Glaucoma, Third Edition*. CRC Press, may 2014, pp. 61–71. [Online]. Available: http://dx.doi.org/10.1201/b16796-7

[3] X. Bian, X. Luo, C. Wang, W. Liu, and X. Lin, "Optic disc and optic cup segmentation based on anatomy guided cascade network," *Computer Methods and Programs in Biomedicine*, vol. 197, p. 105717, 2020.

[4] M. Mokhtari, H. Rabbani, A. Mehri-Dehnavi, R. Kafieh, M.-R. Akhlaghi, M. Pourazizi, and L. Fang, "Local comparison of cup to disc ratio in right and left eyes based on fusion of color fundus images and oct b-scans," *Information Fusion*, vol. 51, pp. 30 – 41, 2019.

[5] A. Septiarini, A. Harjoko, R. Pulungan, and R. Ekantini, "Optic disc and cup segmentation by automatic thresholding with morphological operation for glaucoma evaluation," *Signal, Image and Video Processing*, vol. 11, p. :945–952, 2017.

[6] A. Chakravarty and J. Sivaswamy, "Joint optic disc and cup boundary extraction from monocular fundus images," *Computer Methods and Programs in Biomedicine*, vol. 147, pp. 51 – 61, 2017.

[7] T. Hasegawa, S. Ooto, T. Akagi, T. Kameda, H. Nakanishi, H. O. Ikeda, K. Suda, and A. Tsujikawa, "Expansion of retinal nerve fiber bundle narrowing in glaucoma: An adaptive optics scanning laser ophthalmoscopy study," *American Journal of Ophthalmology Case Reports*, vol. 19, p. 100732, 2020.

[8] A. Ha, Y. K. Kim, and K. H. Park, "Blue-filter fundus photography for detection of retinal nerve fiber layer defect in myopic eyes," *Ophthalmology*, vol. 126, no. 8, p. 1118, 2019.

[9] A. Septiarini, A. Harjoko, R. Pulungan, and R. Ekantini", "Automated detection of retinal nerve fiber layer by texture-based analysis for glaucoma evaluation," *Healthc Inform Res*, vol. 24, no. 4, pp. 335–345, 2018.

[10] R. Panda, N. Puhan, A. Rao, D. Padhy, and G. Panda, "Automated retinal nerve fiber layer defect detection using fundus imaging in glaucoma," *Computerized Medical Imaging and Graphics*, vol. 66, pp. 56 – 65, 2018.

[11] J. Odstrcilik, R. Kolar, R.-P. Tornow, J. Jan, A. Budai, M. Mayer, M. Vodakova, R. Laemmer, M. Lamos, Z. Kuna, J. Gazarek, T. Kubena, P. Cernosek, and M. Ronzhina, "Thickness related textural properties of retinal nerve fiber layer in color fundus images," *Computerized Medical Imaging and Graphics*, vol. 38, no. 6, pp. 508 – 516, 2014.

[12] A. Septiarini, R. Pulungan, A. Harjoko, and R. Ekantini, "Peripapillary atrophy detection in fundus images based on sectors with scan lines approach," in *2018 Third International Conference on Informatics and Computing (ICIC)*, 2018, pp. 1–6.

[13] R. Janani and S. Rajamohana, "Early detection of glaucoma using optic disc and optic cup segmentation: A survey," *Materials Today: Proceedings*, 2021.

[14] P. Elangovan, M. K. Nath, and M. Mishra, "Statistical parameters for glaucoma detection from color fundus images," *Procedia Computer Science*, vol. 171, pp. 2675 – 2683, 2020, third International Conference on Computing and Network Communications (CoCoNet'19).

[15] A. Mvoulana, R. Kachouri, and M. Akil, "Fully automated method for glaucoma screening using robust optic nerve head detection and unsupervised segmentation based cup-to-disc ratio computation in retinal fundus images," *Computerized Medical Imaging and Graphics*, vol. 77, p. 101643, 2019.

[16] A. Septiarini, Hamdani, and D. M. Khairina, "The contour extraction of cup in fundus images for glaucoma detection," *International Journal of Electrical and Computer Engineering*, vol. 6, pp. 2797–2804, 2016.

[17] S. S. Mondal, N. Mandal, A. Singh, and K. K. Singh, "Blood vessel detection from retinal fundas images using gifkcn classifier," *Procedia Computer Science*, vol. 167, pp. 2060 – 2069, 2020, international Conference on Computational Intelligence and Data Science.

[18] S. S. Kar and S. P. Maity, "Blood vessel extraction and optic disc removal using curvelet transform and kernel fuzzy c-means," *Computers in Biology and Medicine*, vol. 70, pp. 174 – 189, 2016.

[19] M. P. Sarathi, M. K. Dutta, A. Singh, and C. M. Travieso, "Blood vessel inpainting based technique for efficient localization and segmentation of optic disc in digital fundus images," *Biomedical Signal Processing and Control*, vol. 25, pp. 108 – 117, 2016.

[20] S. Pathan, P. Kumar, R. Pai, and S. V. Bhandary, "Automated detection of optic disc contours in fundus images using decision tree classifier," *Biocybernetics and Biomedical Engineering*, vol. 40, no. 1, pp. 52 – 64, 2020.

[21] A. Colomer, V. Naranjo, K. Engan, and K. Skretting, "Assessment of sparse-based inpainting for retinal vessel removal," *Signal Processing: Image Communication*, vol. 59, pp. 73 – 82, 2017.

[22] B. Dashtbozorg, A. M. Mendonça, and A. Campilho, "Optic disc segmentation using the sliding band filter," *Computers in Biology and Medicine*, vol. 56, pp. 1 – 12, 2015.

[23] N. E. A. Khalid, N. M. Noor, and N. M. Ariff, "Fuzzy c-means (fcm) for optic cup and disc segmentation with morphological operation," *Procedia Computer Science*, vol. 42, pp. 255 – 262, 2014, medical and Rehabilitation Robotics and Instrumentation (MRRI2013).

[24] G. H. H. Sudhan, R. G. Aravind, K. Gowri, and V. Rajinikanth, "Optic disc segmentation based on otsu's thresholding and level set," in *2017 International Conference on Computer Communication and Informatics (ICCCI)*, 2017, pp. 1–5.

[25] C. Tulasigeri and M. Irulappan, "An advanced thresholding algorithm for diagnosis of glaucoma in fundus images," in *2016 IEEE International Conference on Recent Trends in Electronics, Information Communication Technology (RTEICT)*, 2016, pp. 1676–1680.

[26] J. Almotiri, K. Elleithy, and A. Elleithy, "A multi-anatomical retinal structure segmentation system for automatic eye screening using morphological adaptive fuzzy thresholding," *IEEE Journal of Translational Engineering in Health and Medicine*, vol. 6, pp. 1–23, 2018.

[27] P. S. Mittapalli and G. B. Kande, "Segmentation of optic disk and optic cup from digital fundus images for the assessment of glaucoma," *Biomedical Signal Processing and Control*, vol. 24, pp. 34 – 46, 2016.

[28] A. A, S. W, A. S, R. K, and L. V, "Optic disc segmentation for glaucoma screening system using fundus images," *Clin Ophthalmol*, vol. 1, pp. 2017–2029, 2017.

[29] R. G. Ramani and J. J. Shanthamalar, "Improved image processing techniques for optic disc segmentation in retinal fundus images," *Biomedical Signal Processing and Control*, vol. 58, p. 101832, 2020.

[30] S. T. F. Bokhari, M. Sharif, M. Yasmin, and S. L. Fernandes, "Fundus image segmentation and feature extraction for the detection of glaucoma: A new approach," *Current Medical Imaging*, vol. 14, pp. 77 – 87, 2018.

[31] A. Singh, M. K. Dutta, M. ParthaSarathi, V. Uher, and R. Burget, "Image processing based automatic diagnosis of glaucoma using wavelet features of segmented optic disc from fundus image," *Computer Methods and Programs in Biomedicine*, vol. 124, pp. 108 – 120, 2016.

[32] B. S. Tchinda, D. Tchiotsop, M. NOUBOM, V. Louis-Dorr, and D. Wolf, "Retinal blood vessels segmentation using classical edge detection filters and the neural network," *Informatics in Medicine Unlocked*, p. 100521, 2021.

[33] A. Nithya, A. Appathurai, N. Venkatadri, D. Ramji, and C. Anna Palagan, "Kidney disease detection and segmentation using artificial neural network and multi-kernel k-means clustering for ultrasound images," *Measurement*, vol. 149, p. 106952, 2020.

[34] M. Braiki, A. Benzinou, K. Nasreddine, and N. Hymery, "Automatic human dendritic cells segmentation using k-means clustering and chanvese active contour model," *Computer Methods and Programs in Biomedicine*, vol. 195, p. 105520, 2020.

[35] J. Qiao, X. Cai, Q. Xiao, Z. Chen, P. Kulkarni, C. Ferris, S. Kamarthi, and S. Sridhar, "Data on mri brain lesion segmentation using k-means and gaussian mixture model-expectation maximization," *Data in Brief*, vol. 27, p. 104628, 2019.